



# Scar formation and lack of regeneration in adult and neonatal liver after stromal injury

Ryota Masuzaki, MD, PhD<sup>1</sup>; Sophia R. Zhao, PhD<sup>2</sup>; Eva Csizmadia, PhD<sup>2</sup>; Ioannis Yannas, PhD<sup>3</sup>; Seth J. Karp, MD<sup>1</sup>

1. Department of Surgery, Vanderbilt University Medical Center, Nashville, Tennessee,

2. The Transplant Institute, Beth Israel Deaconess Medical Center, Boston, Massachusetts, and

3. Department of Mechanical and Biological Engineering, Massachusetts Institute of Technology, Cambridge, Massachusetts

## Reprint requests:

Dr. S. J. Karp, Vanderbilt Medical School,  
909 Oxford House, 1313 21st Avenue  
South, Nashville, TN 37232-4761, USA.  
Tel: +1 615 936 8989;  
Fax: +1 615 936 8999;  
Email: seth.karp@vanderbilt.edu

Manuscript received: February 9, 2012

Accepted in final form: September 25,  
2012

DOI:10.1111/j.1524-475X.2012.00868.x

## ABSTRACT

Known as a uniquely regenerative tissue, the liver shows a remarkable capacity to heal without scarring after many types of acute injury. In contrast, during chronic liver disease, the liver responds with fibrosis, which can progress to cirrhosis and ultimately liver failure. The cause of this shift from a nonfibrotic to a fibrotic response is unknown. We hypothesized that stromal injury is a key event that prevents restoration of normal liver architecture. To test this, we developed a model of stromal injury using a surgical incision through the normal liver in adult and neonatal mice. This injury produces minimal cell death but locally complete stromal (extracellular matrix) disruption. The adult liver responds with inflammation and stellate cell activation, culminating in fibrosis characterized by collagen deposition. This sequence of events is remarkably similar to the fibrotic response leading to cirrhosis. Studies in neonates reveal a similar fibrotic response to a stromal injury. These findings suggest that extracellular matrix disruption leads not to regeneration but rather to scar, similar to other mammalian organs. These findings may shed light on the pathogenesis of chronic liver disease, and suggest therapeutic strategies.

Long known as a uniquely regenerative organ, the liver can restore its mass and functional capacity even in response to massive tissue loss. In addition, after acute but nonlethal injury, for example after acetaminophen overdose, acute hepatitis A, or alcohol toxicity, the liver parenchyma heals without scar or functional consequence.<sup>1</sup>

In stark contrast, however, is the response of the liver to chronic injury. In the setting of hepatitis C, long-term alcoholic abuse, metabolic diseases, autoimmune diseases, or certain congenital abnormalities, the liver responds with fibrosis. Progression may lead to cirrhosis and eventually liver failure as massive deposition of extracellular matrix (ECM) compromises synthetic and excretory functions.<sup>2,3</sup>

What is unique about chronic injury that causes scarring? One possibility is that parenchymal (hepatocyte) injury and stromal (extracellular matrix [ECM]) injury are distinct and elicit disparate responses from the liver. Under this hypothesis, the liver heals an acute hepatocyte insult without fibrosis, whereas ongoing insult damages the ECM, causing irreversible damage.

Resolving this question has implications for the development of therapeutic options that have been successful in other tissues. For example, in both skin and peripheral nerve, an understanding of wound injury led to the fabrication of bioengineered scaffolds that promote regenerative healing by inhibiting fibrosis and scar formation. These studies ultimately led to the development of Food and Drug Administration (FDA)-approved products to induce regeneration in both tissues.<sup>4-9</sup>

Other sets of studies examining early fetal injury show profound differences in the healing response compared with adult tissues, with early fetal skin being capable of healing without significant scarring.<sup>10</sup> A recent report shows that in neonatal mice, even the heart can repair itself without significant scarring, an ability lost by 7 days of age.<sup>11</sup> At least some of the difference between fetal and adult healing may be due to differences in wound contraction and myofibroblast function.<sup>12</sup>

To address the fundamental question of how adult and fetal liver respond to a stromal injury, we created a model of stromal disruption in both adult and neonatal mice and demonstrate that both respond with scar, similar to other tissues. These results provide a basic understanding of the response of the liver to injury and may provide guidance for therapeutic interventions.

## MATERIALS AND METHODS

### Mice

All mice used for experiments were male C57BL/6. Adults were approximately 8 weeks of age. Neonatal mice were 2

ECM  
H & E  
BrdU

Extracellular matrix  
Hematoxylin and eosin  
Bromodeoxyuridine

days old (p2). All mice were obtained from Jackson Laboratories (Bar Harbor, ME). All experiments were performed at least in triplicate and all photomicrographs are representative samples.

### Mouse liver stromal injury model

All surgeries were performed according to the National Institutes of Health guidelines for the humane treatment of laboratory animals and with approval of the Harvard or Vanderbilt Institutional Animal Care and Use Committee depending on the location of the experiments. In experiments on adult mice, anesthesia was achieved with 60 mg/kg ketamine (Hospira, Lake Forest, IL) and 7 mg/kg xylazine (Phoenix Pharmaceutical, Burlingame, CA). A small incision was then made below the right costal margin. The liver was identified and an incision was made through the liver parenchyma using a scissors. This injury was 1 cm long and went completely through the liver. The abdomen was then closed in two layers. Mice were recovered and monitored for pain and activity. In experiments on neonatal mice, anesthesia was achieved by cooling the pups on an ice bed for 4 minutes as described.<sup>11</sup> An incision of less than 1 cm was made below the right costal margin and the liver was exposed. An incision of less than 1 cm was made in the right lobe of the liver. The abdomen was closed in one layer. Mice were sacrificed in accordance with institutional guidelines at appropriate intervals as described.

### Histopathology

Livers were removed and fixed in 10% buffered formalin, embedded in paraffin, sectioned, and stained with hematoxylin and eosin (H&E).

Immunohistochemical studies were performed on paraffin-embedded liver tissue according to standard protocols. Antibodies used were: rat anti-human CD3 (1:100, Serotec, Raleigh, NC), rat-anti mouse CD45B220 (1:100, BD Pharmingen, San Jose, CA), rabbit anti-mouse collagen I (1:200, Novus, Littleton, CO), polyclonal rabbit anti-SM22 alpha (1:100, Abcam, Cambridge, MA), rat anti-mouse Gr-1 (1:200, BD Pharmingen), polyclonal rabbit anti-GFAP (1:800, Dako, Carpinteria, CA), and polyclonal rabbit anti-vimentin (1:500, Novus).

Immunofluorescence was performed on paraffin sections. Fluorescence double staining was performed using paraffin-embedded tissue and detected with a bromodeoxyuridine (BrdU) kit (1:50; BD Biosciences, San Jose, CA), polyclonal goat anti-HNF-4 $\alpha$  (1:100; Santa Cruz, Santa Cruz, CA), or polyclonal goat anti-albumin antibodies (1:50, Santa Cruz).

Sirius Red staining was performed using paraffin sections as previously described.<sup>13</sup> After deparaffinization, nuclei were stained using Weigert's hematoxylin for 8 minutes. Collagen was stained by using a Sirius Red/picric acid solution (Sirius Red # 365548, Sigma-Aldrich, St. Louis, MO) for 1 hour and washed in two changes of acidified water. Tissue was dehydrated in 100% ethanol and slides were cleared in xylene and mounted.

### Image analysis

MetaMorph software (Universal Imaging Corporation, Sunnyvale, CA) was used to quantitate the stained areas, which are

denoted % area stained on the ordinate axis. Color development times for immunohistochemical detection were held constant to ensure consistent MetaMorph detection of the stained area. Color thresholding was used to distinguish the stained, colored area. Percentages of threshold area in total area were calculated and compared among the group.

### Statistics

*p*-Values were calculated using the Student's *t*-test. *p*-Values of less than or equal to 0.05 were considered significant.

## RESULTS

### Histology and scar formation

In order to describe the response of the adult liver to injury, a 1 cm through and through longitudinal incision was made in the liver of 8-week-old male mice and examined at various time points after injury. There were no deaths as a result of the injury. H&E shows the progression of the healing response (Figure 1A–F, scar area outlined in blue). By 6 hours after injury, a necrotic zone forms at the area of injury (Figure 1A). By 24 hours, the clot is beginning to organize and there is central tissue loss (Figure 1B). By 48 hours, the clot has organized and a surrounding basophilic infiltrate is apparent (Figure 1C). At 4 days, the clot has become more organized and the infiltrate persists (Figure 1D). By 7 days, cellular architecture is restored, and the parenchyma is contracting at the site of injury (Figure 1E). Finally, by 28 days, the contraction is complete and the area of injury is recellularized (Figure 1F). Over a period of 1 month, therefore, the liver undergoes a response typical of tissues in the body in response to a stromal injury (reviewed in Yannas<sup>14</sup>): inflammation with reestablishment of parenchymal or epithelial tissue integrity and scar formation.

At the conclusion of the healing process, the liver parenchyma appears recellularized by H&E staining. To better understand the critical events in the response to injury, we used a variety of stains and immunohistochemical analysis. We first looked at collagen I, which is an important component of scar in cirrhotic liver<sup>2</sup> (Figure 2A–C, top graph, Supporting Information Figure S1). At 6 hours after injury, there is no collagen deposition (Figure 2A). By 48 hours, however, collagen is beginning to be laid down at the periphery of the injury. Four days after injury, collagen I deposition is pronounced in two lines which represent the limits of the area of inflammation (Figure 2B, arrows). By 7 days, the collagen surrounding the injury coalesces into a single line, which persists to 28 days (Figure 2C). Quantitation of staining reveals marked increase to 4 days that stabilizes by 28 days (Figure 2, top graph).

To confirm these results, we used the collagen stain Sirius Red for the area of injury (Figure 2D–F, bottom graph, Supporting Information Figure S2). Similar to our data with collagen I immunostaining, Sirius Red staining is absent at 6 hours and increases by 4 days after injury in an area that surrounds the injury site (Figure 2D). By 7 days and continuing through 28 days, the area of injury is well demarcated as a linear scar with surrounding contraction of parenchymal and stromal tissues (Figure 2F). Quantitation of staining reveals an increase to 4 days followed by stabilization to 28 days

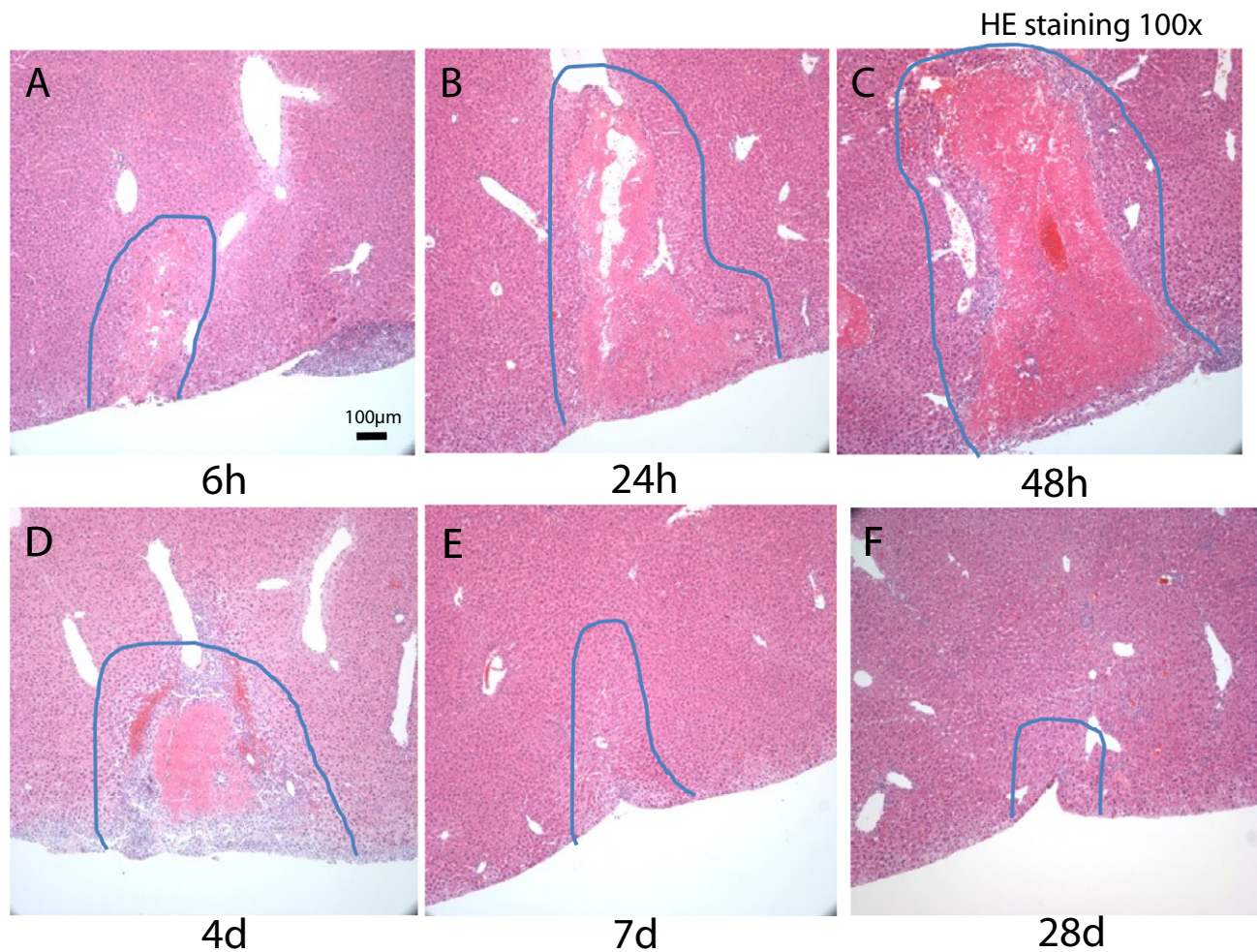


**Figure 1.** Histologic response to stromal liver injury in adult mice over time. Hematoxylin and eosin staining after injury shows initial area of injury (A) which gives rise to a necrotic area at 24 hours (B). A clot organizes and is ringed by infiltrating cells 48 hours after injury (C), which further consolidates by 4 days (D). By 7 days (E) and 28 days (F), there is little histologic residual from the injury. Magnification 100x.

(Figure 2, bottom graph). Taken together, these results show the deposition of collagen and therefore scar formation along the tract of the injury.

### Proliferative response

Liver injury in the form of hepatocyte death or tissue loss is a stimulus for hepatocyte proliferation. To determine whether stromal injury with minimal hepatocyte destruction is mitogenic for hepatocytes, BrdU was injected 2 hours prior to sacrifice in a series of injured animals. Staining for BrdU at various times after injury revealed the patterns of cellular proliferation (Figure 3). Six hours after the injury, few cells have infiltrated into the injury area and there is minimal proliferation (Figure 3A). By 48 hours, the edge of the injury contains small cells, many of which are proliferating, and this continues through 4 days (Figure 3B, graph, and Figure S3).

By 7 days there is minimal proliferation, which is virtually absent by 14 days (Figure 3, graph, and Supporting Information Figure S3).

To determine which, if any, of these proliferating cells were hepatocytes, double fluorescence immunostaining was performed for the hepatocyte marker HNF4 $\alpha$  (red) and BrdU (green, indicating proliferation) (Figure 4). There are no hepatocytes within the scar area (Figure 4A). To determine which of the proliferating cells were hepatocytes, double staining for HNF4 $\alpha$  and BrdU showed two cells that stained for both, indicating the presence of proliferating hepatocytes (Figure 4B, arrows). To confirm these results, sections were double stained for albumin and BrdU and examined using immunofluorescence. Proliferating cells outside the scar are identified as hepatocytes by red cytoplasmic staining (albumin) and green nuclear staining (BrdU) (Figure 4C).

In normal, unstressed liver, very few hepatocytes proliferate. These results, therefore, suggest that local injury provides

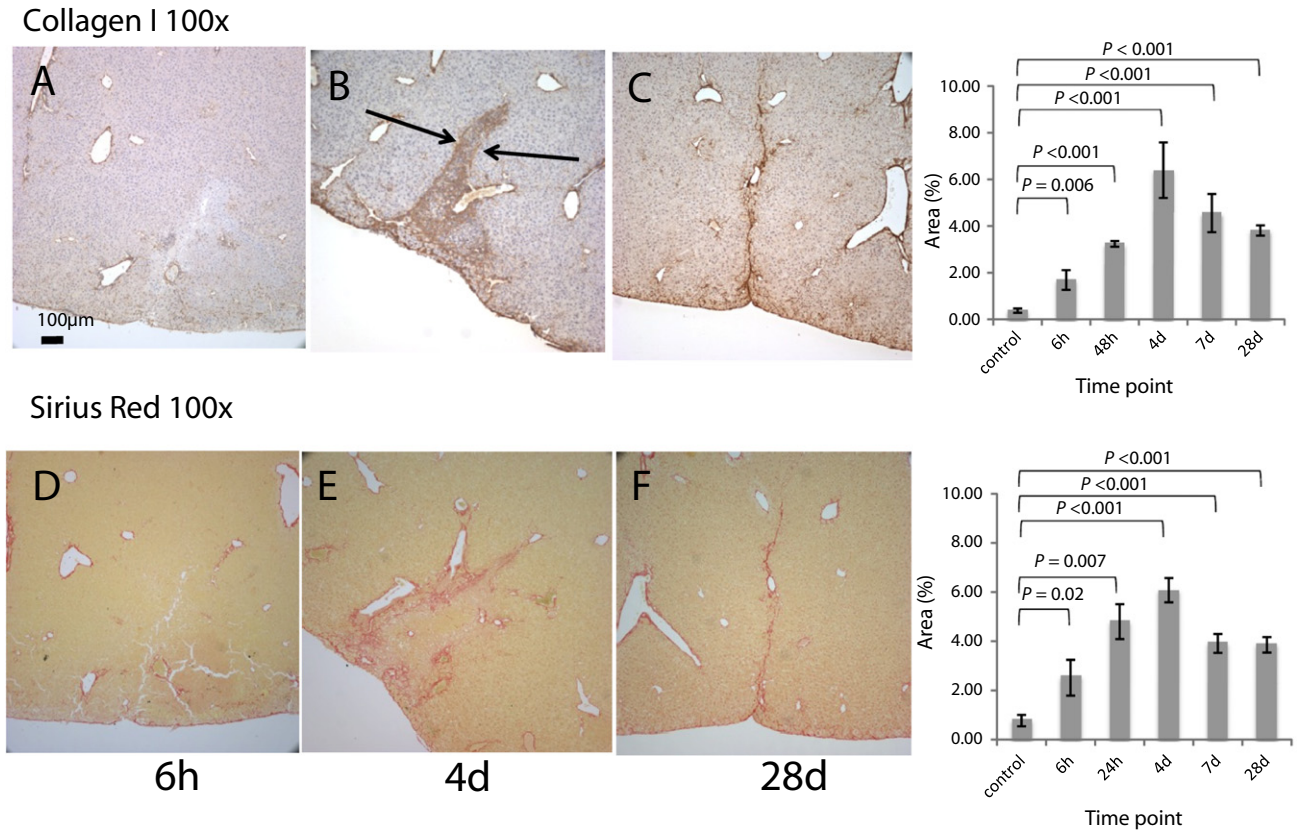


**Figure 2.** Collagen deposition and Sirius Red staining over time in response to stromal injury. Immunohistochemistry shows no collagen deposition 6 hours after the injury (A). By 4 days, staining occurs in a double line pattern flanking the injury (arrows, B). By 28 days, the double line has coalesced into a single line and the parenchyma contracts (C). Quantitation shows increasing staining to 4 days with modest decrease thereafter (top graph). Sirius Red reveals a similar pattern. Six hours after injury, there is no staining (D). Four days after injury, there is a double pattern that coalesces in a single line by 28 days (E,F). Quantitation shows increasing staining to 4 days with modest decrease thereafter (bottom graph).

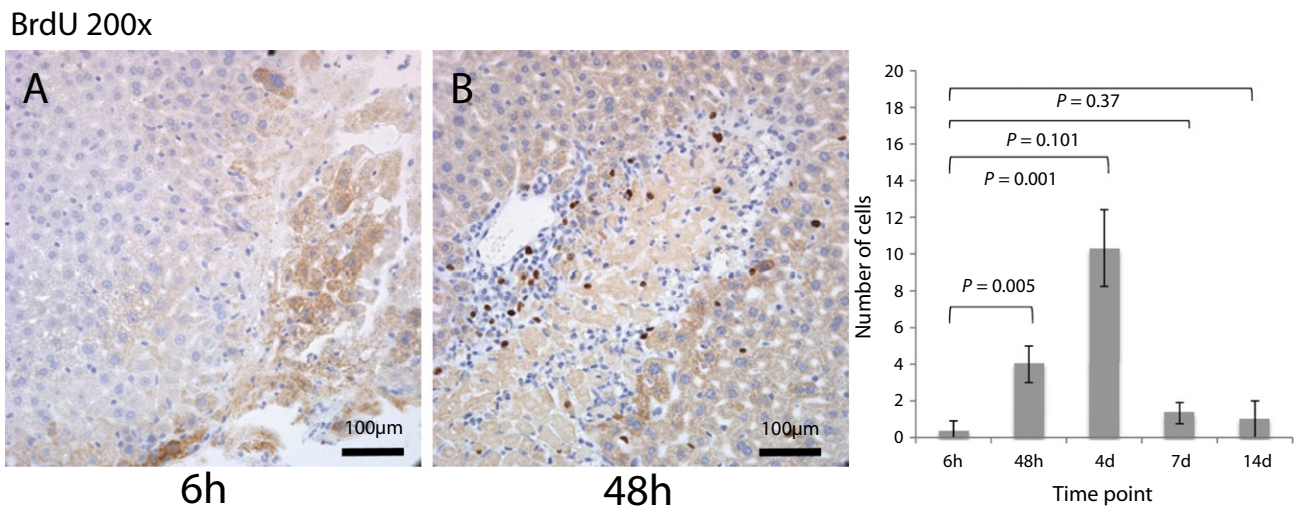


**Figure 3.** Proliferation around the area of injury after stromal injury. BrdU incorporation reveals no proliferating cells 6 hours after injury (A). By 48 hours, many cells in the area stain for BrdU (B, brown nuclear staining), which continues at 4 days after injury and then decreases by 14 days after injury (graph). BrdU, bromodeoxyuridine.

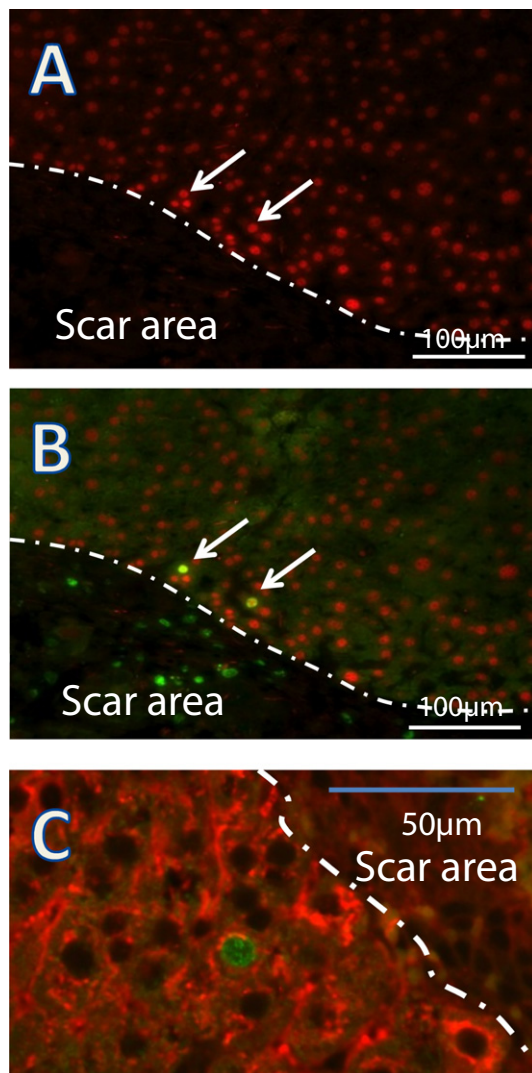


**Figure 4.** Proliferation around the area of injury. Double staining fluorescence immunohistochemistry reveals hepatocyte nuclei around area of injury by HNF4 $\alpha$  staining (A, red nuclei). Cells in the area outside the scar stain for both HNF4 $\alpha$  and BrdU (B, green, arrows). Proliferating cells (green nuclei) outside the scar also stain for albumin in the cytoplasm (C, red staining).

a mild local stimulus to hepatocyte proliferation, but that most of the proliferating cells are part of the inflammatory infiltrate.

#### Nature of the response to stromal injury

To further determine the nature of the inflammatory infiltrate, we performed immunohistochemistry for Gr-1, a granulocyte marker (Figure 5). As expected, there are no granulocytes present prior to injury (Figure 5A). By 6 hours, however, there is a significant infiltrate that persists to 4 days (Figure 5B and graph). Fourteen days after injury, the inflammatory infiltrate

is no longer present (Figure 5 graph and Supporting Information Figure S4). These results show a granulocyte response typical of injury in many other types of tissue.

To further characterize the nature of the inflammatory infiltrate, we looked for T-cells using antibodies to CD3, and B cells using the marker CD4B220. Neither showed significant changes from baseline after liver injury (data not shown).

Stellate cells activation is thought to be a critical event in the initiation of liver fibrosis during chronic disease.<sup>15</sup> To compare the mechanism of fibrosis seen in our model to that of chronic disease, we examined GFAP, a marker of quiescent stellate cells, and Vimentin, markers of stellate cell activation. GFAP stains heterogeneously over 14 days, peaking at 4 days (Figure 6A,B, graph, Supporting Information Figure S5), suggesting a recruitment of quiescent stellate cells. Markers of stellate cell activation also change significantly. For sm22, at baseline there is minimal staining (Figure 7A). By 6 hours after injury, however, there is increased staining at the area of injury, and by 48 hours and 4 days after there is significant staining around the area of the injury. By 14 days after injury, the stellate cell pattern reverts to normal (Figure 7B and graph, Supporting Information Figure S6). Vimentin follows a similar pattern. Prior to injury, there is diffuse staining (Figure 8A). By 48 hours, there is increased staining which continues to increase at 4 days and then returns to normal by 14 days (Figure 8B and graph, Supporting Information Figure S7). These results suggest that stellate cell activation is a feature of fibrosis in response to stromal injury, similar to the process in chronic liver disease.

#### Fetal response to stromal injury

In contrast to injured adult tissue, fetal injuries can sometimes heal without scar formation.<sup>12</sup> To examine this, we adapted our adult model to neonatal (p2) liver. After a linear injury, neonatal mice showed a pattern of injury and healing similar to adult mice. An area of necrosis at 48 hours is followed by reestablishment of the parenchyma with contraction by 28 days after injury (Figure 9A, B). Sirius Red confirmed a fibrotic scar across the tract of injury that was pronounced at 28 days (Figure 9C, graph).

## DISCUSSION

To determine the response of the liver to a stromal injury, we set up and investigated a mouse model of stromal disruption in which an incision was made in the liver of adult and neonatal mice. This injury preferentially disrupts the ECM with only local cellular injury. Initially, an area of hemorrhage and necrosis forms. This region is infiltrated within 6 hours by granulocytes that form a typical inflammatory reaction. Two days after injury, stellate cells are widely activated, and by 4 days after injury, fibrosis ensues, and persists through at least 1 month after the injury. This limited injury is weakly mitogenic for nearby hepatocytes.

These findings suggest that a stromal injury, even a limited one, generates a fibrotic response from the liver. This is in marked contrast to the response of the liver to a direct and even massive acute hepatocyte toxicity or removal of a lobe without a true stromal injury. In both of these cases, there is no significant fibrosis. These results are significant because they suggest that stromal (ECM) and parenchymal injuries elicit disparate responses.

Gr-1 200x

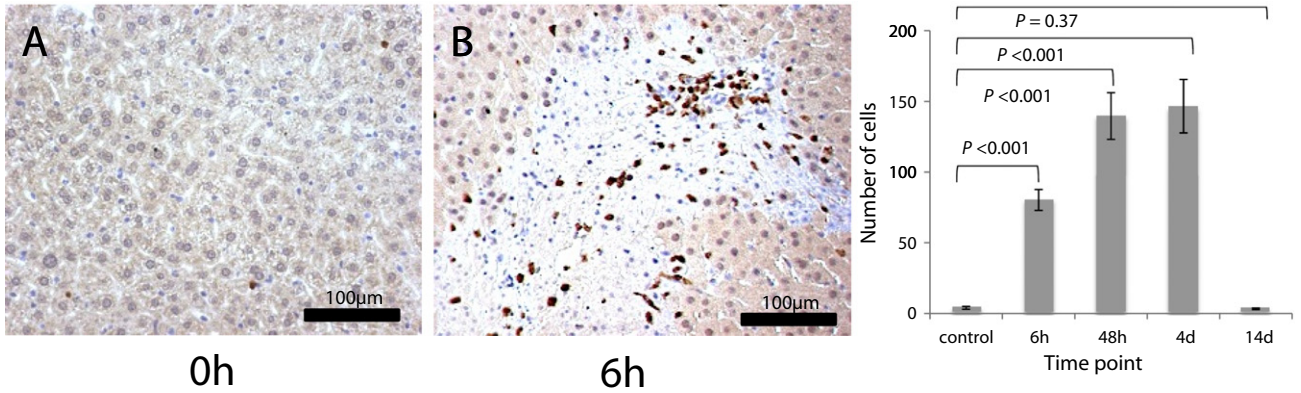


**Figure 5.** Granulocyte response to stromal injury. Immunohistochemistry for GR-1 shows no neutrophils prior to injury (A). Six hours after injury, neutrophils have infiltrated the area of injury (B). These persist through 48 hours and 4 days and are gone by 14 days (graph).

GFAP 200x

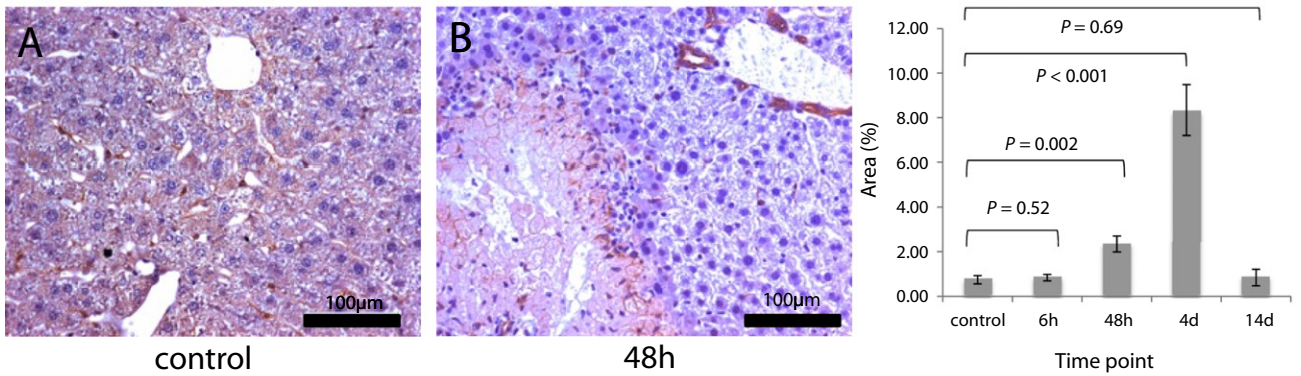


**Figure 6.** Quiescent stellate cells after injury. Immunohistochemistry for the quiescent stellate cell marker GFAP. Between 0 and 48 hours after injury (A,B), staining gradually increases. After a peak at 4 days, staining returns to normal (graph).

Sm22 200x

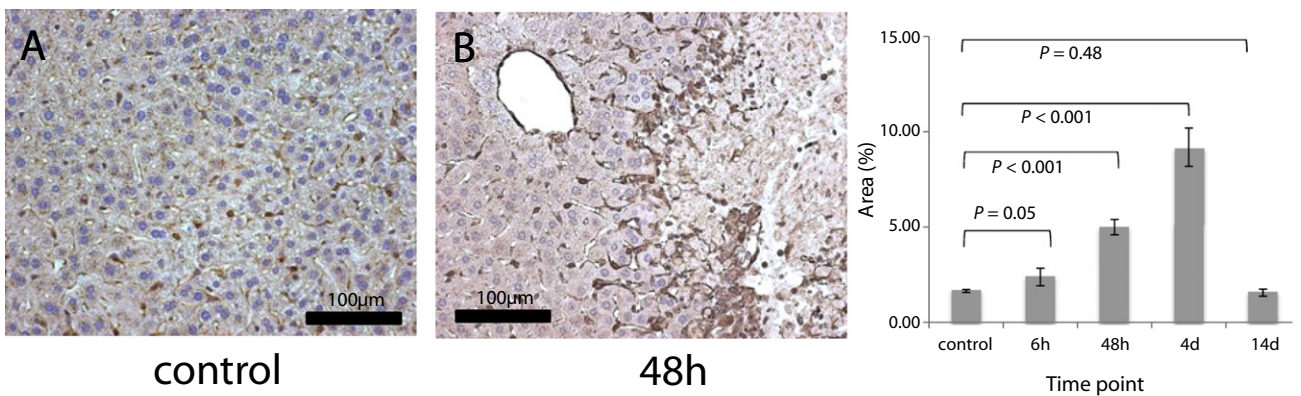


**Figure 7.** Stellate cell activation in response to stromal injury using SM-22. Immunohistochemistry for SM-22 shows low-level staining prior to injury (A). By 48 hours after injury, stellate cells become activated at the edge of the lesion (B, brown staining). Intensity increases by 4 days and then returns to baseline by 14 days (graph).

Vimentin 200x

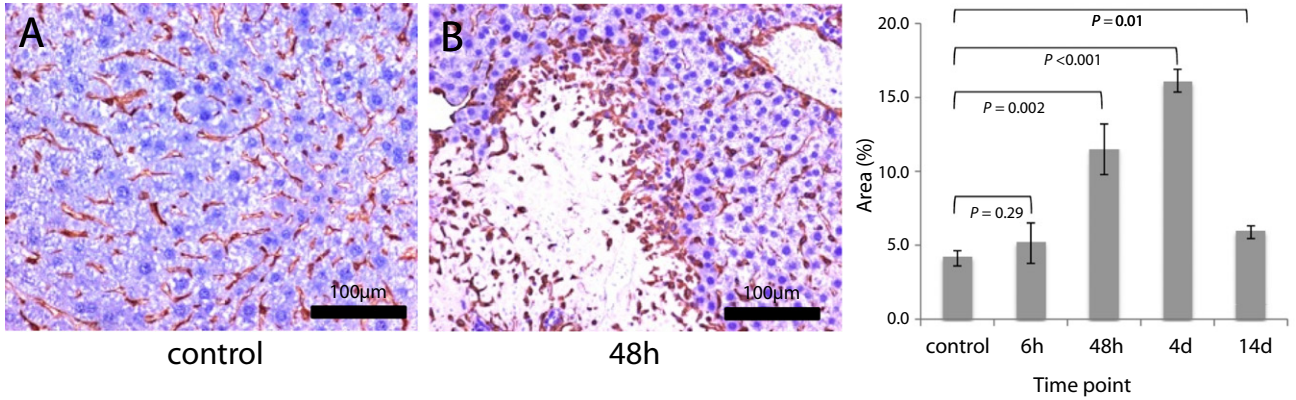


**Figure 8.** Stellate cell activation in response to stromal injury using Vimentin. Immunohistochemistry for Vimentin shows a similar pattern to sm22. There is diffuse staining at baseline (A), which increases by 48 hours (B). Staining intensity peaks at 4 days and then decreases by 14 days (graph).

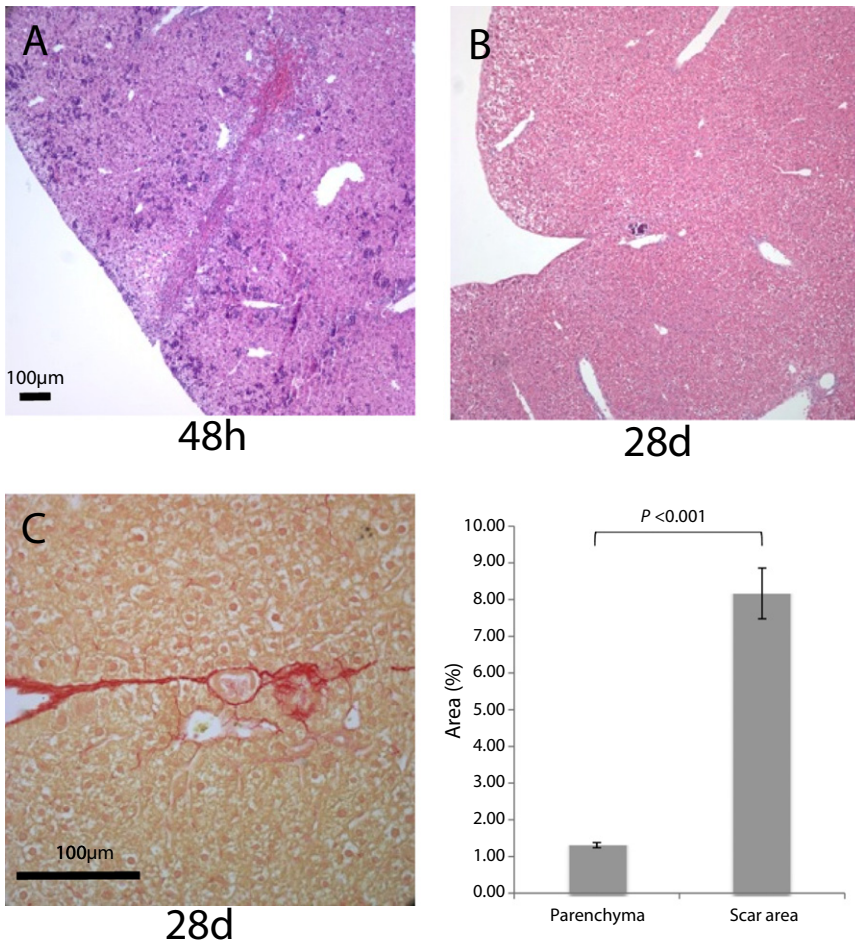


**Figure 9.** Histologic progression of stromal liver injury in neonatal (p2) mice over time. Hematoxylin and eosin staining after injury shows initial area of injury at 48 hours (A). By 28 days, the parenchyma has contracted and there is little histologic residual from the injury (B). Sirius Red staining shows scar formation at 28 days after injury (C, graph).

A fundamental question in liver disease is to explain the switch from a nonfibrotic to a fibrotic response in the setting of chronic injury. As hepatocytes are able to repopulate the liver ad infinitum for all practical purposes, it is unclear as to why ongoing hepatocyte injury should result in cirrhosis and liver failure.<sup>16</sup> Historically, fibrosis has been convincingly attributed to inflammation and TGF- $\beta$ 1 signaling, with its effects on matrix components and matrix metalloproteinases.<sup>17</sup> Intimately involved in the processes, stellate cells play a role in contraction and the release of vasoactive substances.<sup>2</sup> Nevertheless, how these pathways are activated remains unclear.

Our results are consistent with these well-known findings, while at the same time suggesting that stromal injury is sufficient to initiate the fibrotic response. This response to stromal disruption we observe in our model can be summarized by an inflammatory response, stellate cell activation, and reestablishment of tissue integrity by scar formation characterized by deposition of collagen I. This sequence of events is exactly the same as occurs during the development of liver fibrosis on the way to cirrhosis. These results are therefore consistent with the hypothesis that stromal (ECM) injury is a critical event in the development of chronic liver disease. Importantly, this may occur as a result of ongoing inflammation that is the consequence of hepatocyte injury.

As our model of stromal disruption is characterized by significant inflammation, we cannot distinguish whether it is the stromal injury or the inflammation is essential for fibrosis. Other findings, however, shed light on this question. Many forms of acute liver disease are accompanied by significant inflammation but ultimately do not produce a fibrotic response. For example, ischemia-reperfusion injury elicits quite a strong inflammatory response,<sup>18</sup> as does alcoholic hepatitis and acetaminophen overdose.<sup>19,20</sup> If inflammation was the critical event in fibrosis, these insults would lead to fibrosis, which they do not, at least as acute events. It is therefore more likely that stromal disruption is the key event, though we cannot exclude that the fibrosis depends on the intensity, chronicity, or cellular makeup of the inflammation. Furthermore, many reports describe regression of fibrosis over time.<sup>21</sup> The permanence of the fibrosis in our model is unknown to further than 1 month out, though there does not seem to be improvement from 2 to 4 weeks. Taken together, these findings potentially represent a new way to understand chronic liver disease. Combined with our previous data that the liver does not recapitulate embryonic signaling patterns after mass loss, these data suggest that the liver is not the uniquely regenerative organ it has been thought to be.<sup>22</sup>

In addition to similarity with chronic liver disease, our model shows that the response of the liver to stromal injury is remarkably similar to the injury response in many other tissues. For example, in skin, inflammation occurs and fibroblasts deposit and remodel collagen, resulting in a scar.<sup>23</sup> Likewise, after myocardial injury, inflammation and cardiac fibroblasts play a key role in scar formation.<sup>24</sup>

Important reports show that neonatal skin and heart can regenerate without scarring.<sup>10,11</sup> We examined this specifically in neonatal liver and were surprised to find that neonatal liver scarred just like adult liver. In our model, therefore, there is no evidence that the neonatal liver is a privileged site for nonfibrotic healing. It is possible that had we injured the liver at an earlier stage, we might find no scar formation. The role of stellate cells in this process has not been evaluated.

There are a number of clinically relevant implications of these studies. Work on implantable scaffolds to inhibit scar and encourage regeneration has led to FDA-approved devices for skin and nerve regeneration.<sup>4,5,8,23,25</sup> Other studies show that implantation of a scaffold with neural stem cells into an adult rat spinal injury model significantly improves functional recovery compared with cells alone.<sup>26</sup> A similar strategy applied to the liver could have clinical utility. Use of a scaffold to drive regeneration of even limited amounts of functional liver tissue might be enough to ameliorate clinical symptoms including enzyme deficiency or coagulopathy. To begin to consider these types of treatments, the fundamental response of the liver to a simple injury must be understood. Takimoto et al. have demonstrated that use of a scaffold in the liver can serve as a substrate for liver regeneration.<sup>27</sup> Future studies will examine the ability of an engineered scaffold to support hepatocyte ingrowth.

Another possible application of these studies is to use this simple injury model as a quick and cost-effective test of antifibrotic agents in the liver. To do this, it will be necessary to determine to what extent this model is directly relevant to the global fibrosis that occurs over time in response to chronic liver injury.

These studies show that the liver is not the privileged organ it was once thought to be and paints a picture of a much more common response to injury. Even minimal disruption in the ECM is a serious and irreversible problem. These findings help reveal fundamental biology of the response of the liver to injury, and may lead to strategies to treat human disease.

## ACKNOWLEDGMENTS

This work was supported by grants from the Center for Integration of Medicine and Innovative Technology at the Massachusetts Institute of Technology, the Transplant Center of the Beth Israel Deaconess Medical Center, and Vanderbilt University Medical Center.

*Conflict of Interest:* There are no conflicts of interest.

## REFERENCES

1. Iredale JP. Hepatic stellate cell behavior during resolution of liver injury. *Semin Liver Dis* 2001; 21: 427–36.
2. Friedman SL. Molecular regulation of hepatic fibrosis, an integrated cellular response to tissue injury. *J Biol Chem* 2000; 275: 2247–50.
3. Schuppan D. Structure of the extracellular matrix in normal and fibrotic liver: collagens and glycoproteins. *Semin Liver Dis* 1990; 10: 1–10.
4. Yannas IV, Burke JF, Orgill DP, Skrabut EM. Wound tissue can utilize a polymeric template to synthesize a functional extension of skin. *Science* 1982; 215: 174–6.
5. Yannas IV, Lee E, Orgill DP, Skrabut EM, Murphy GF. Synthesis and characterization of a model extracellular matrix that induces partial regeneration of adult mammalian skin. *Proc Natl Acad Sci U S A* 1989; 86: 933–7.
6. Murphy GF, Orgill DP, Yannas IV. Partial dermal regeneration is induced by biodegradable collagen-glycosaminoglycan grafts. *Lab Invest* 1990; 62: 305–13.
7. Hsu WC, Spilker MH, Yannas IV, Rubin PA. Inhibition of conjunctival scarring and contraction by a porous collagen-glycosaminoglycan implant. *Invest Ophthalmol Vis Sci* 2000; 41: 2404–11.

8. Chamberlain LJ, Yannas IV, Hsu HP, Strichartz G, Spector M. Collagen-GAG substrate enhances the quality of nerve regeneration through collagen tubes up to level of autograft. *Exp Neurol* 1998; 154: 315–29.
9. Chamberlain LJ, Yannas IV, Hsu HP, Strichartz GR, Spector M. Near-terminus axonal structure and function following rat sciatic nerve regeneration through a collagen-GAG matrix in a ten-millimeter gap. *J Neurosci Res* 2000; 60: 666–77.
10. Longaker MT, Whitby DJ, Adzick NS, Crombleholme TM, Langer JC, Duncan BW, Bradley SM, Stern R, Ferguson MW, Harrison MR. Studies in fetal wound healing: VI second and early third trimester fetal wounds demonstrate rapid collagen deposition without scar formation. *J Pediatr Surg* 1990; 25: 63–8.
11. Porrello ER, Mahmoud AI, Simpson E, Hill JA, Richardson JA, Olson EN, Sadek HA. Transient regenerative potential of the neonatal mouse heart. *Science* 2011; 331: 1078–80.
12. Yannas IV. Similarities and differences between induced organ regeneration in adults and early foetal regeneration. *J R Soc Interface* 2005; 2: 403–17.
13. Junqueira LC, Bignolas G, Brentani RR. Picrosirius staining plus polarization microscopy, a specific method for collagen detection in tissue sections. *Histochem J* 1979; 11: 447–55.
14. Yannas IV. *Tissue and organ regeneration in adults*. New York: Springer, 2001.
15. Mormone E, George J, Nieto N. Molecular pathogenesis of hepatic fibrosis and current therapeutic approaches. *Chem Biol Interact* 2011; 193: 225–31.
16. Overturf K, al-Dhalimy M, Ou CN, Finegold M, Grompe M. Serial transplantation reveals the stem-cell-like regenerative potential of adult mouse hepatocytes. *Am J Pathol* 1997; 151: 1273–80.
17. Henderson NC, Iredale JP. Liver fibrosis: cellular mechanisms of progression and resolution. *Clin Sci* 2007; 112: 265–80.
18. Jaeschke H. Reactive oxygen and mechanisms of inflammatory liver injury. *J Gastroenterol Hepatol* 2000; 15: 718–24.
19. Bautista A. Neutrophilic infiltration in alcoholic hepatitis. *Alcohol* 2002; 27: 17–21.
20. Lawson JA, Farhood A, Hopper RD, Bajt ML, Jaeschke H. The hepatic inflammatory response after acetaminophen overdose: role of neutrophils. *Toxicol Sci* 2000; 54: 509–16.
21. Shiratori Y, Imazeki F, Moriyama M, Yano M, Arakawa Y, Yokosuka O, Kuroki T, Nishiguchi S, Sata M, Yamada G, Fujiyama S, Yoshida H, Omata M. Histologic improvement of fibrosis in patients with hepatitis C who have sustained response to interferon therapy. *Ann Intern Med* 2000; 132: 517–24.
22. Otu HH, Naxerova K, Ho K, Can H, Nesbitt N, Libermann TA, Karp SJ. Restoration of liver mass after injury requires proliferative and not embryonic transcriptional patterns. *J Biol Chem* 2007; 282: 11197–204.
23. Yannas IV, Hill BJ. Selection of biomaterials for peripheral nerve regeneration using data from the nerve chamber model. *Biomaterials* 2004; 25: 1593–600.
24. Palatinus JA, Rhatt JM, Gourdie RG. Translational lessons from scarless healing of cutaneous wounds and regenerative repair of the myocardium. *J Mol Cell Cardiol* 2010; 48: 550–7.
25. Yannas IV, Orgill DP, Burke JF. Template for skin regeneration. *Plast Reconstr Surg* 2011; 127 (Suppl. 1): 60S–70S.
26. Teng YD, Lavik EB, Qu X, Park KI, Ourednik J, Zurakowski D, Langer R, Snyder EY. Functional recovery following traumatic spinal cord injury mediated by a unique polymer scaffold seeded with neural stem cells. *Proc Natl Acad Sci U S A* 2002; 99: 3024–9.
27. Takimoto Y, Dixit V, Arthur M, Gitnick G. De novo liver tissue formation in rats using a novel collagen-polypropylene scaffold. *Cell Transplant* 2003; 12: 413–21.

## Supporting Information

Additional Supporting Information may be found in the online version of this article:

**Figure S1.** Collagen deposition over time in response to stromal injury. Immunohistochemistry shows no collagen deposition 6 hours after injury (A). By 48 hours after injury, diffuse staining for collagen I is present (arrow, B), which becomes more intense by 4 days in a double line pattern flanking the injury (arrows, C). By 7 days, the double line has coalesced into a single line (arrows, D) and the parenchyma contracts (circle, D). The pattern persists at 28 days (E). Magnification 100×.

**Figure S2.** Sirius Red staining over time in response to stromal injury. Sirius Red staining shows no fibrosis 6 or 24 hours after injury (A,B). By 4 days, there is a double line pattern (C), which coalesces into a single line by 7 days (D) and 28 days (E). This pattern is similar to collagen I staining. Magnification 100×.

**Figure S3.** Proliferation around the area of injury after stromal injury. BrdU incorporation reveals no proliferating cells 6 hours after injury (A). By 48 hours, many cells in the area stain for BrdU (B, brown nuclear staining), which continues at 4 days after injury (C). By 7 days and continuing to 14 days, there are few proliferating cells (D,E). Magnification 400×.

**Figure S4.** Granulocyte response to stromal injury. Immunohistochemistry for GR-1 shows no neutrophils prior to injury (A). Six hours after injury, neutrophils have infiltrated the area of injury (B). These persist through 48 hours and 4 days (C,D) and are gone by 14 days (E). Magnification 400×.

**Figure S5.** Quiescent stellate cells after injury. Immunohistochemistry for the quiescent stellate cell marker GFAP. Between 0 and 14 days after injury, staining remains diffuse. Magnification 200×.

**Figure S6.** Stellate cell activation in response to stromal injury. Immunohistochemistry for SM-22 shows low level staining prior to injury (A). Six hours after injury, stellate cells become activated (B, brown staining), which becomes more intense at the edge of the injury by 48 hours and 4 days after the injury (C,D). By 14 days after the injury, activated cells are gone (E). Magnification 400×.

**Figure S7.** Stellate cell activation in response to stromal injury using vimentin. Immunohistochemistry for the stellate cell activation marker vimentin shows a similar pattern to SM-22. There is occasional staining at baseline (A), which increases by 48 hours and 4 days (B–D) and which takes on a linear pattern at 14 days (E). Magnification 400×.